Water-Rock Interactions, Ore Deposits, and Environmental Geochemistry: A Tribute to David A. Crerar
© The Geochemical Society, Special Publication No. 7, 2002
Editors: Roland Hellmann and Scott A. Wood

Experimental calibration of metastable plagioclase-epidote-fluid equilibria at elevated temperatures and pressures: Applications to the chemistry of hydrothermal fluids at mid-ocean ridges

WILLIAM E. SEYFRIED[1], JR., KANG DING[1], AND BIN RAO[2]

[1]Department of Geology and Geophysics, University of Minnesota, Minneapolis, MN, 55455 USA
[2]Department of Earth Science, Nanjing University, Nanjing, P.R. China
e-mail: wes@maroon.tc.umn.edu

Abstract—Mineral solubility experiments were conducted to assess phase relations in the CaO-Na_2O-Al_2O_3-SiO_2-Fe_2O_3-FeO-CuO-Au-H_2O-H_2S-HCl system at elevated temperatures, pressures and dissolved Cl^- concentrations. An important objective of this study was to compare measured concentrations of aqueous species with those predicted from constraints imposed by fluid-mineral equilibria. Mineral phases including plagioclase and epidote solid solutions, together with anhydrite, magnetite, pyrite chalcopyrite and quartz were used to buffer activities of key components of the system. These phases were chosen because they can be directly or indirectly linked to phase relations in subseafloor reaction zones at mid-ocean ridges.

Temperature and dissolved Cl^- concentrations were observed to play important roles in the direction and magnitude of chemical exchange. Increasing temperature from 400 to 425 °C caused most species to increase in concentration, although dissolved Ca decreased. At a given temperature and pressure, an increase in dissolved Cl^- resulted in sharp increases in dissolved Ca, Fe, and Cu, while dissolved gases (H_2, H_2S) decreased as a consequence of salting-out effects. Decreasing pressure from 500 to 300 bars again resulted in a decrease in dissolved Ca, whereas concentration of other major dissolved species increased.

Experimental results are in good agreement with theoretical predictions of fluid chemistry when compositional constraints imposed by metastable plagioclase and epidote solid solutions are explicitly taken into account. Indeed, temperature-dependent changes in dissolved Ca and Na are consistent with metastable plagioclase (An_{70})-fluid equilibria at quartz-saturation, while pH (in-situ) values, are consistent with constraints imposed by metastable epidote-fluid equilibria. Metastable mineral-fluid equilibria is also indicated by dissolved metal concentrations, in particular Fe, Cu and Au. At a dissolved Cl^- concentration of 1.0 molal, pH (in-situ) values of 5.07 and 4.77 are estimated for fluids from experiments at 425 and 400 °C, 500 bars, respectively. As shown here and elsewhere, slight changes in pH (in-situ) result in relatively large changes in dissolved Fe and Cu concentrations at experimental conditions. Measured concentrations of dissolved Al are considerably in excess of theoretical predictions, although in good agreement with recent data from hot spring vents.

Whereas pH and dissolved metal concentrations are highly sensitive to constraints imposed by the composition of plagioclase and epidote solid solutions, dissolved H_2S is affected less by these constraints. Thus, experimentally calibrated vent fluid $H_2S(aq)$ concentrations can be used to constrain the redox evolution of subseafloor reaction zones at mid-ocean ridges. Relatively low $H_2S(aq)$ concentrations of some vent fluids either indicate low temperatures or the absence of pyrite in subseafloor reaction zones.

The generally good agreement between experimental and theoretical models depicting complex hydrothermal alteration processes provides a measure of the recent progress that has been made in theoretical geochemistry and justifies the use of these models to constrain alteration processes in subseafloor reaction zones at mid-ocean ridges.

1. INTRODUCTION

Over the past decades a substantial body of data has accumulated that indicates the effectiveness of mineral dissolution/precipitation processes in controlling the chemistry of hot spring vent fluids at mid-ocean ridges. In particular, investigations of vent fluids at EPR 21°N (Von Damm et al., 1985; Campbell et al., 1988a), EPR 9-10°N (Von Damm et al., 1997), Juan de Fuca Ridge (Von Damm, 1988; Butterfield et al., 1994; Butterfield and Massoth, 1994), MARK and TAG (Campbell et al., 1988b; Edmond et al., 1995), and at the Lucky Strike field, Mid-Atlantic Ridge (Von Damm et al., 1998), reveal dissolved concentrations of aqueous species that are largely consistent with phase equilibria control in subseafloor reaction zones at elevated temperatures and pressures. That many of these studies also involve time-series observations, which often indicate steady-state conditions of dissolved species (e.g., see Campbell et al., 1988a; Edmond et al. 1995), provides added support for subseafloor processes involving mineral-fluid equilibria at reaction zone conditions. Even vent fluids that reveal relatively recent changes in temperature, pressure and salinity owing to subseafloor mixing and phase separation effects (e.g., EPR 9-10°N, Von Damm et al., 1997; Fornari et al., 1998), reveal corresponding changes in fluid chemistry largely in keeping with mineral-fluid phase equilibria controls. For example, "F-vent" at EPR 9°N, which was sampled in 1991 and 1994, where large scale changes in temperature and dissolved Cl^- were observed, also reveals systematic and predictable changes in dissolved metals, H_2 and H_2S, suggesting rock-buffering of vent fluid chemistry. Not only are phase equilibria constraints consistent with dissolved concentrations of the major- and trace-element chemistry of the vent fluid, but also with the temporal variability of hydrogen and oxygen isotopes (Shanks et al., 1995; Berndt et al., 1996; Von Damm et al., 1997).

Experimental and theoretical investigations of fluid-mineral equilibria at elevated temperatures and pressures are obviously needed to constrain reactions that control pH, redox and metal mobility in subseafloor hydrothermal systems (Bowers et al., 1988; Berndt et al., 1989; Seyfried et al., 1991). For example, Berndt and Seyfried (1993) showed that metastable plagioclase feldspar (An60-70)-fluid equilibria at temperatures and pressures of 400 °C and 400 bars, respectively, are needed to account for the relatively high dissolved Ca concentrations and Ca-Na-SiO_2 systematics of hot spring vent fluids. Moreover, Ding and Seyfried (1992b) and Seyfried and Ding (1993, 1995) performed a series of redox- and pH-buffered experiments in the K_2O-Na_2O-Al_2O_3-SiO_2-Fe_2O_3-FeO-CuO-H_2O-H_2S-HCl system to determine thermodynamic data for Cu-chloro complexes over a wide range of conditions. These results, together with previous experimental data (Ding and Seyfried, 1992a), were used to constrain redox conditions in subseafloor reaction zones. Indeed, results of these studies suggest that pH and redox conditions are often buffered by an assemblage of minerals composed of calcic-plagioclase, epidote, quartz, magnetite, anhydrite and pyrite (Seyfried and Ding, 1995). The likely existence of anhydrite as a reactant in subseafloor reaction zones was a surprising result of these experiments, although in keeping with sulfur isotope data and dissolved SO_4^{2-} concentrations in carefully sampled hot spring fluids (Shanks et al., 1995; Von Damm, 1995 and references therein). Although it is unlikely that this complete assemblage of minerals applies to all reaction zones at mid-ocean ridges, it almost certainly does in systems where the permeability allows seawater-derived sulfate to penetrate deeply into the crust, and where sufficient rock-fluid interaction occurs to cause the elimination of pyrrhotite as a primary reactant in basalt/gabbro.

In addition to simulating hydrothermal alteration processes at mid-ocean ridges, mineral-fluid equilibria experiments, involving anhydrite, and plagioclase and epidote solid solutions, afford a means to assess the role of key variables on metal mobility and dissolved gas concentrations for an intermediate redox state, and thus supplement the large body of experimental data available for more oxidizing and reducing systems. Moreover, owing to recent advances in theoretical geochemistry, results of thermodynamic models can be directly compared with the experimental solubility measurements. In this way, the general accuracy of predictive models can be verified lending confidence to the applicability of these models as a means to assess key aspects of subseafloor hydrothermal alteration processes. Similarly, theoretical data can be used to constrain experimental measurements and point out non-equilibrium effects, such as metastable states, which may control one or more components of the fluid phase. For example, we have already established the role of plagioclase metastability (Berndt and Seyfried, 1993) on Ca^{2+}/Na^+ exchange in Cl^--bearing aqueous fluids at elevated temperatures and pressures, and it is likely that other phases behave similarly. Indeed, the common occurrence of zoned crystals of epidote from subareal geothermal systems and results from epidote-bearing experiments (Liou, 1973; Bird and Helgeson, 1980a,b) suggest this may be the case for this phase as well. Thus, in the present study, fluid chemistry coexisting with plagioclase and epidote solid solutions, quartz, magnetite, anhydrite, pyrite, and chalcopyrite was measured and monitored at 400 to 425 °C and 500 to 300 bars in 0.53 and 1.0 molal total dissolved Cl^- solutions. Additionally, the inherent compositional variability of trace elements in the natural minerals used for the experiments, together with constraints imposed by the composition of the reaction cell (Au), allowed us to assess qualitatively the effect of Cl^-, redox, pH and temperature on the mobility of key trace elements. This in turn helps to constrain further the potential mobility of these species during subseafloor hydrothermal alteration processes.

2. METHODS

2.1. Experimental and Analytical Techniques

Mineral solubility experiments were performed using flexible gold reaction cells (Seyfried et al., 1987). A major advantage of the flexible cell system is that it allows internally filtered fluid samples to be withdrawn at experimental conditions, thus mitigating quench effects for most dissolved species.

Reactants used for the experiments reported here were all natural minerals: coarse crystalline plagioclase and epidote solid solution, quartz, magnetite, anhydrite, pyrite, and chalcopyrite. All minerals were obtained from the mineral collections at the University of Minnesota or Wards Natural Science Establishment. Prior to use, the minerals were acid-cleaned and ground in an agate ball mill, and then sieved through nylon mesh to recover the 74 to 149 micron size fractions. X-ray diffraction, optical microscope examination, electron microprobe analysis and bulk chemical analysis by ICP-MS were performed on the starting solids to constrain mineral compositions. The mole fraction of the anorthite and epidote components of plagioclase and epidote solid solution were determined to be approximately 0.7 and 0.45 respectively (Table 1), whereas all other minerals were nearly pure phases.

Each experiment consisted of a charge containing approximately 30 g plagioclase solid solution, 9 g of epidote solid solution, 7 g of quartz, 12 g of magnetite, 8 g of anhydrite, 16 g of pyrite, and 4 g of chalcopyrite (Table 2). These minerals were placed in a 150-mL Au reaction cell with approximately 100 g of Na-Ca-Cl fluid. The relative abundance of plagioclase, in particular, was used to enhance the rate of approach to plagioclase-quartz-fluid equilibria (see below).

All experiments were designed in accordance with the Gibbs phase rule. As a consequence of this, mineral phases, components and imposed constraints were balanced so as to buffer completely the distribution of aqueous species, assuming, of course, full thermodynamic equilibrium. For example, in their study of plagioclase-quartz-fluid equilibria, Berndt and Seyfried (1993) showed that at a given temperature, pressure, dissolved Cl^- and plagioclase composition, the chemical system was invariant. Moreover,

Table 1. Chemical composition of plagioclase and epidote solid solutions used for hydrothermal experiments. Analyses performed by ICP-MS following fusion with lithium-metaborate and dissolution in HCl (see text).

Oxide (wt. %)	**Plagioclase-ss**	**Epidote-ss**
SiO_2	51.23	38.90
TiO_2	0.00	0.00
Al_2O_3	31.43	29.14
Cr_2O_3	0.00	0.00
Fe_2O_3	0.00	0.00
FeO_t	0.41	6.67
MnO	0.00	0.00
MgO	0.17	0.00
CaO	14.29	23.84
Na_2O	3.29	0.00
K_2O	0.00	0.00
H_2O	0.05	0.80
Totals	100.87	100.0
Mol %	An = 70	Ep = 45

Table 2. Abundances in grams of mineral phases used for hydrothermal experiments performed at 0.53 and 1.0 molal total dissolved chloride. Temperatures and pressures ranged from 400-425 °C and 300-500 bars respectively.

Mineral Phases	**0.53 molal Series(g)**	**1.0 molal Series(g)**
Plagioclase (An70)	30.15	30.32
Quartz	7.01	7.11
Epidote (Ep45)	9.33	9.34
Anhydrite	8.00	8.01
Magnetite	12.08	12.35
Pyrite	15.98	16.07
Chalcopyrite	4.13	4.37

Table 3. Chemical composition of fluid samples taken during fluid-mineral equilibria experiments at temperatures of 400° and 425 °C, 300-500 bars and 0.53 molal total dissolved Cl. The designator, na, indicates species not analyzed in a particular fluid sample owing to sample size constraints.

Temp		**400**	**400**	**400**	**400**	**425**	**425**
Pressure		**500**	**500**	**400**	**300**	**500**	**400**
Reaction Time (hrs.)	**Start**	**720**	**2880**	**336**	**350**	**1200**	**1000**
$H_{2(aq)}$(mm)	0	na	0.18	0.25	0.37	0.53	0.67
$H_2S_{(aq)}$(mm)	0	na	8.9	10	12	15	21
SO_4^{2-}(mm)	0	<0.30	0.13	na	0.20	0.41	0.19
Cl(mm)	532	557	547	559	548	579	555
SiO_2(mm)	0	23	22	20	17	24	19
Na(mm)	472	493	480	496	489	503	531
Ca(mm)	30	29	28	27	25	24	20
Fe(mm)	0	3.9	4.1	4.2	5.6	7.3	9.1
Cu(μm)	0	75	na	77	77	100	na
Au(μm)	0	0.3	na	0.2	na	na	na
Ni(μm)	0	1.7	na	1.2	0.8	na	na
Pb(μm)	0	8.0	na	8.3	na	na	na
Al(μm)	0	94.1	16	13	13	na	6

Table 4. Chemical composition of fluid samples taken during fluid-mineral equilibria experiments at temperatures of 400° and 425 °C, 500 bars and 1.0 molal total dissolved Cl. As noted, the designator, na, indicates species not analyzed in a particular fluid sample owing to sample size constraints.

Temp		**400**	**400**	**425**	**425**
Pressure		**500**	**500**	**500**	**500**
Reaction Time (hrs.)		**300**	**2160**	**336**	**2000**
$H_{2(aq)}$(mm)	0	na	0.17	0.42	0.49
$H_2S_{(aq)}$(mm)	0	na	7.4	14	15
SO_4^{2-}(mm)	0	na	0.41	0.42	0.43
Cl(mm)	1021	1030	1050	996	1075
SiO_2(mm)	0	21.0	21	23	22.0
Na(mm)	809	863	850	821	855
Ca(mm)	102	82	80	77	78
Fe(mm)	0	9.85	11	25	26
Cu(μm)	0	98.9	116	185	190
Au(μm)	0	0.36	0.39	0.24	0.26
Ni(μm)	0	na	12	6	14
Pb(μm)	0	5.8	6.2	4.9	6.3
Al(μm)	0	19	20	29	15

their study showed that an ideal solid solution model for plagioclase accounted best for the chemistry of fluids coexisting with An_{60} and An_{82} plagioclase at 400 °C, 400 bars. For Fe- and S-bearing systems, however, as is the case here, redox constraints must be imposed to achieve this same state of invariance. In effect, for a given plagioclase composition, total dissolved Cl^- (charge-balance constraint), temperature and pressure, inclusion of four other mineral phases (e.g., magnetite, pyrite, anhydrite, chalcopyrite) is needed to buffer completely the ten-component system, (Na_2O-CaO-SiO_2-Al_2O_3-FeO-Fe_2O_3-CuO-HCl-H_2O-H_2S), including the composition of epidote solid solution. That the present series of experiments involves epidote solid solution with a specific composition (Table 1) necessarily creates a metastable condition unless this phase recrystallizes completely to a composition consistent with imposed redox constraints (see Bird and Helgeson, 1980a,b). As noted earlier, it is likely that epidote solid solution, like plagioclase, may not recrystallize sufficiently on experimental time scales to achieve full thermodynamic equilibrium. Whether or not epidote composition achieves equilibrium can be established unambiguously, however, from measured fluid chemistry and by comparison of the composition of epidote solid solution before and after the experiments.

Two series of experiments were performed. The first series was conducted at temperatures of 400 to 425 °C, pressures of 300 to 500 bars and 0.53 molal total dissolved Cl^-, while the second was at 1.0 m Cl^- and temperatures and pressures of 400-425 °C and 500 bars, respectively. Reaction progress was evaluated by time-series measurements, which tended to show that steady-state conditions were achieved (Table 3, 4). Steady state and equilibrium, of course, can be quite different. Here, however, we made use of a sampling strategy established previously by Berndt and Seyfried (1993) for their plagioclase-quartz-fluid experiments at conditions virtually identical to those of the present study. In particular, Berndt and Seyfried (1993) showed that metastable plagioclase-fluid equilibria could be effectively established after relatively short reaction periods when the direction of approach to equilibrium was in the Ca-consuming direction, a finding in keeping with much earlier results by Orville (1972). Thus, all of the experiments performed as part of the present investigation were conducted with a starting fluid having "excess" Ca, reactants with "excess" plagioclase, and with reaction times more than necessary to achieve equilibrium as established by Berndt and Seyfried (1993). Although not directly reversing plagioclase exchange reactions created some ambiguity with respect to establishing an equilibrium condition, this was offset by the need to conserve fluid sample to complete the relatively large number of analyses of aqueous species needed to assess the ten-component system under investigation. Dissolved gas measurements, together with determination of trace metal species, such as Cu, Pb and Au, which required a separate procedure for fluid sampling and analysis, placed severe constraints on the inventory of fluid sample from any given experiment.

Fluid samples were analyzed for Na, Si, Ca, Fe, Cu, Al, Pb, Ni, and Au by ICP-MS, while Cl^-, SO_4^{2-} and H_2S (the latter converted to SO_4^{2-} following oxidation by treatment with heated H_2O_2) were analyzed by ion chromatography. Dissolved H_2 was determined by gas chromatography.

Although the source of many of the major and minor elements in solution can clearly be linked to primary components of the starting solids or aqueous fluid, many of the trace elements in solution are derived from dissolution of trace elements in these same solids. The exception, of course, is gold, which was derived from the gold reaction cell. Even though the concentrations of trace elements in the experimental system are different from those in phases in sub-seafloor settings, the observed changes in the dissolved concentrations of these species (e.g., Pb, Ni, Au) as a function of temperature, pressure and dissolved Cl^- during the experiments can still provide valuable insight on the mobility of these species during subseafloor hydrothermal alteration processes.

The accuracy of reported concentrations of major dissolved cations and anions (mmolal concentrations) is approximately 2%, and 10-20% for trace element species (μmolal concentrations), at the 95% confidence level. The upper range of uncertainty for trace elements largely results from the nature of the sampling process used for these species, which often required dissolution of a metal-bearing precipitate produced during the sampling process (see Seewald and Seyfried, 1990; Seyfried and Ding, 1993). The accuracy of reported concentrations of dissolved gases (H_2 and H_2S) is approximately 10% at the 95% confidence level. Analytical uncertainties given for all aqueous species are based on processing of replicate samples from the experiments and from results of previous research in our lab involving mineral-fluid equilibria studies at a similar range of conditions.

The pH was not measured on fluid samples from the experiments owing to the effects of sulfide mineral precipitation during sample processing, which renders pH values highly uncertain. The pH, of course, could be calculated for fluids from the experiments by making use of phase equilibria constraints as discussed by Ding and Seyfried (1992a). Dissolved metals and $H_2S(aq)$ are sampled separately into acidified solutions in gas-tight syringes to preclude the effects of mineralization on the measured inventory of these species.

2.2. Theoretical Constraints

Mineral solubility calculations were performed at the same temperatures, pressures and total dissolved Cl^- concentrations as used for the experiments to better assess hydrothermal alteration processes. Not only do these calculations constrain experimental results, but also the experiments in turn provide insight into the relative accuracy of theoretical models of fluid-mineral equilibria at elevated temperatures pressures and dissolved Cl^- concentrations.

The standard state adopted in this study for all mineral phases and liquid water is unit activity of the pure phase at the temperature and pressure of interest. For aqueous ions and complexes, the standard state is unit activity of the species in a hypothetical one-molal solution, referenced to infinite dilution in H_2O at the pressure and temperature of the experiment. Accordingly, the activity of H_2O and activity coefficients for solute species approach unity at infinite dilution at any pressure and temperature of interest. Individual molal activity coefficients for charged species (γ_i) were calculated using the B-dot equation of Helgeson (1969).

For neutral species, activity coefficients were calculated from the Setchénow equation:

$$\log \gamma_n = b_{\gamma,n} I \qquad (1)$$

where $b_{\gamma,n}$ is a temperature- and pressure-dependent coefficient characteristic of the nth neutral species and the electrolyte composition (Chen and Marshall, 1982), and I, the true ionic strength, which takes explicit account of the distribution of aqueous species. Ding and Seyfried (1990), for example, determined Setchénow coefficients for $H_{2(aq)}$ and $H_2S_{(aq)}$ in NaCl fluids at temperatures and pressures from 300 to 450 °C and 300 to 500 bars respectively by determining the dissolved concentration of H_2 and H_2S as a function of NaCl concentration in fluids coexisting with pyrite-pyrrhotite-magnetite. Data show that Setchénow coefficients for H_2 and H_2S increase dramatically with decreasing pressure and increasing temperature. Thus, for the range of conditions applicable to the present study, γ_{H_2} and γ_{H_2S} of between 1.2 and 1.5 are indicated, the higher values corresponding to higher dissolved NaCl and temperature, and lower pressure. The existence of species other than NaCl in the fluid has not been accounted for, however, and it is likely that dissolved salts, such as $CaCl_2$ and $FeCl_2$ join NaCl in contributing to the activity/concentration relations for neutral species. This certainly is a concern, but an even greater concern involves the virtual absence of any data for activity coefficients for HCl°, NaCl° and NaOH° at temperatures and pressures in excess of 300 °C and steam saturation, respectively. Thus, for these and similar species, activity coefficients were assigned a constant value of 1.2, in keeping with previous conventions (Ding and Seyfried, 1992a and references therein).

In addition to activity coefficient data for aqueous species, assessment of fluid-mineral equilibria at elevated temperatures and pressures requires detailed knowledge of hydrolysis constants for minerals, activity-composition relations for minerals, where solid solution effects are important, together with dissociation constant data for all aqueous complexes. These data coupled with appropriate mass-balance, mass-action and charge-balance constraints permit determination of the distribution of aqueous species, which then can be compared with results of experimental studies (Ding and Seyfried, 1992a,b; Seyfried and Ding, 1995). In this study, thermodynamic data used for minerals, ions, and gases are from SUPCRT92 (Johnson et al., 1992), whereas data for most aqueous complexes, which are consistent with the SUPCRT92 database, are from Sverjensky et al. (1991, 1997). These data are based on the revised HKF (Helgeson et al., 1981) equations of state for aqueous species (Tanger and Helgeson, 1988; Shock and Helgeson, 1988; 1990; Shock et al., 1989;

Shock et al., 1997) and correlations among equation of state parameters and standard partial molal properties at 25 °C and 1 bar. In addition to these data, however, experimental mineral solubility-data from Ding and Seyfried (1992a,b) were used to obtain stability constants for $FeCl_2°_{(aq)}$ and $CuCl°_{(aq)}$. In the past (see Saccocia and Seyfried, 1990; Seyfried et al., 1991), a Newton-Raphson iterative technique was used to solve simultaneously the full range of mass-action, mass-balance and charge-balance relations needed to assess mineral-fluid equilibria. In this particular case, however, we made use of the EQ3/EQ6 software package (Wolery and Daveler, 1992), which was modified by us to allow calculations to be performed at the same range of conditions as for the experiments. Solid solutions in EQ3/EQ6 are treated with ideal mixing models. Thus, an ideal molecular mixing model was used to define the activities of components of plagioclase solid solution, in keeping with results of Berndt and Seyfried (1993), while an ideal site mixing model was used to express activity-mole fraction relations for epidote and clinozoisite components of epidote solid solution, in keeping with data and interpretations of Bird and Helgeson (1980a,b). This mixing model accounts for the temperature dependence of substitutional order-disorder of Al^{+3} and Fe^{+3} in the M1 and M3 octahedral sites in epidote solid solutions.

3. RESULTS

3.1. Fluid Chemistry

3.1.1. Major elements (Ca, Na, Fe, $SiO_2(aq)$)

Dissolved Ca concentrations decreased from starting conditions to those in fluids at elevated temperatures and pressures for both 0.53 and 1.0 molal Cl^- experiments (Table 3 and 4). Indeed, Ca removal from solution is largely balanced by gains in dissolved Na and Fe. In general, Ca for Na and Fe exchange tend to increase with decreasing pressure and increasing temperature (Table 3 and 4). Moreover, data show that for the redox condition maintained during the experiment, which is intermediate between PPM (pyrite-pyrrhotite-magnetite) and HMP (hematite-magnetite-pyrite), changes in dissolved Cl^- induce large-scale changes in dissolved Fe (Fig. 1), with lesser changes in dissolved Ca and Na. As will be discussed at greater length below, these effects are entirely consistent with formation of aqueous Fe-bearing chloro-complexes at the range of pH and redox conditions fixed by mineral-fluid equilibria at the temperatures and pressures of the experiments (Seyfried and Ding, 1993).

Owing to the presence of quartz, the dissolved concentration of SiO_2 tended to increase with increasing temperature and to decrease with decreasing pressure, consistent with quartz-fluid equilibria. For example, at 400 °C, dissolved SiO_2 decreased systematically from 23 to 16.5 mmolal with decreasing pressure from 500 to 300 bars respectively (Table 3). A similar trend can be seen for the 425 °C series of experiments (0.53 m Cl^-), but here the pressure drop did not extend below 400 bars.

3.1.2. Dissolved gases (H_2 and H_2S) and SO_4^{2-}

Owing to the well-known effect of temperature, pressure and dissolved Cl^- on mineral solubility and activity-concentration relations in the FeO-Fe_2O_3-H_2S-H_2O-HCl system (Ding and Seyfried, 1989; Ding and Seyfried, 1992a,b; Seyfried and Ding, 1995), it is not surprising that dissolved H_2 and H_2S changed significantly during the experiments. Indeed, the dissolved concentration of both gases increased with increasing temperature and decreasing pressures (Tables 3 and 4). At the elevated temperatures and pressures of the experiments, however, salting-out effects are particularly robust (Ding and Seyfried, 1989). It is not surprising, therefore, that the concentrations of H_2 and H_2S tended to decrease with increasing dissolved Cl^- (Fig. 1). Dissolved SO_4^{2-}, in contrast, failed to reveal a clear trend with temperature and pressure, but appeared to increase with increasing dissolved Na (Table 3 and 4), which may reflect formation of $NaSO_4^-{}_{(aq)}$, but this needs to be established better with additional experiments or modeling calculations.

3.1.3. Minor elements (Cu, Au, Ni, Pb and Al)

Dissolved Cu concentrations reveal large-scale changes during the experiments (Table 3 and 4, Fig. 1). As with most minerals, the solubility of chalcopyrite (primary reactant) is greatly affected by temperature, pressure, redox, Cl^- and pH (Crerar and Barnes, 1976; Hemley et al., 1992; Ding and Seyfried, 1992b; Seyfried and Ding, 1993). At 1.0 molal total dissolved Cl^-, for example, a temperature increase from 400 to 425 °C caused Cu concentration to increase significantly. The effect of pressure on dissolved Cu concentrations, however, was relatively modest at the temperatures investigated. It is not entirely clear whether this is real or apparent, being caused entirely or in part by analytical uncertainties related to Cu measurements at relatively low levels where these effects can be relatively large (Seewald and Seyfried, 1990; Seyfried and Ding, 1995).

As noted previously, we also measured the dissolved concentrations of Au, Ni, Pb and Al during the experiments, although sample-size limitations and

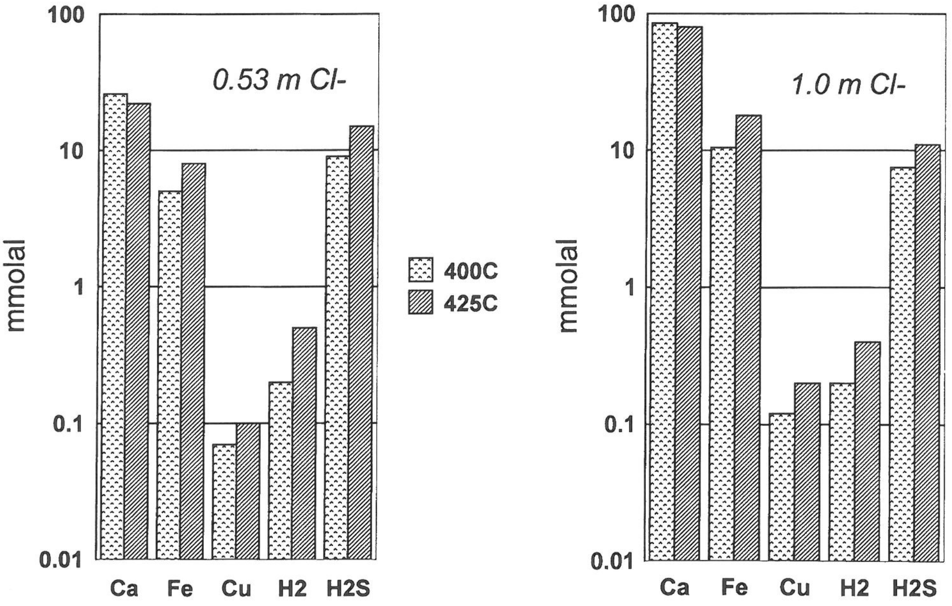

Figure 1. Experimentally determined dissolved Ca, Fe, Cu, H_2, and H_2S in 0.53 m Cl$^-$ (A) and 1.0 m Cl$^-$ (B) fluid coexisting with plagioclase-epidote-quartz-magnetite-anhydrite-pyrite-chalcopyrite assemblage at 400 and 425 °C, 500 bars.

sampling procedures often precluded analysis of all fluid samples for each of these species. Owing to the trace quantities of the source phases (see above), however, we were not able to determine unambiguously mineralogical controls, although results of SEM and EDX analyses of bulk alteration products revealed Ni and Pb associated with both sulfide and oxide. Data which are available for Ni reveal a slight negative pressure effect, something like Cu. Nickel also tended to increase with increasing Cl$^-$ (Table 3 and 4). Lead, in contrast, increased slightly with decreasing pressure (500 to 400 bars only), but failed to record any other unambiguous changes with temperature or dissolved Cl (Table 3, 4), in spite of the existence of well-known chloro-complexes of Pb, which are very much temperature-dependent (Hemley et al., 1992). Possibly, the very small amounts of Pb in the starting solids precluded sufficient mass transfer between solid and aqueous phases to confirm these aqueous speciation effects. In contrast, Au decreased with temperature increase from 400 to 425 °C (1 molal Cl$^-$), although, again, insufficient data are available to assess unambiguously the role of other key variables, a modest pressure effect notwithstanding.

The dissolved concentration of Al generally falls in the range of approximately 10-20 μmolal, and like the other trace elements (Pb, Au, Ni), it is difficult to demonstrate unambiguous correlations with temperature, pressure and dissolved Cl$^-$. The dissolved Al concentration of the first sample from the experiment performed at 400 °C, 500 bars and 0.53 m Cl$^-$, however, is unusually high (94 μm), which may be caused by sample contamination or early-stage non-stoichiometric dissolution effects. That the Al concentration of the subsequent sample from this experiment decreased to a value more typical of other fluid samples from other experiments leads us to question the earlier result. In any event, it is likely that the average dissolved concentration of Al (10-20 μm) reflects control by the bulk assemblage of aluminosilicate phases used as reactants for the experiments.

3.2. Mineral Chemistry

The solid run products from all experiments were examined optically and petrographically, as well as by X-ray diffraction and electron microprobe to evaluate changes in the composition of the starting mineral assemblage. In general, all of the starting minerals were observed at the end of all of the experiments, although there were changes in grain size and crystallinity suggesting mineral dissolution and reprecipitation and crystal growth. In addition, micro-

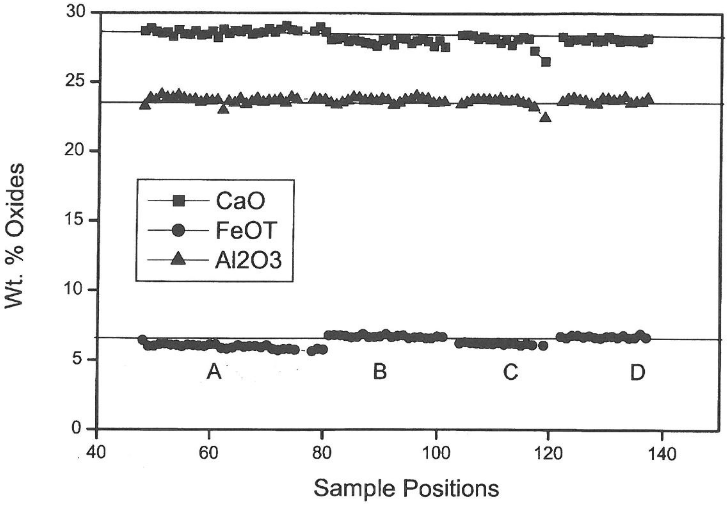

Figure 2. Electron microprobe analyses (CaO, Al_2O_3, FeO) of four (A through D) epidote grains from experiment at 425 °C, 500 bars and 1.0 m Cl^-. Data reveal compositions virtually identical to starting values (solid lines) determined by wet chemical techniques (see text and Table 1). Sample positions refer to transect locations across mineral grains. These data are representative of all samples from all experiments, and indicate existence of metastable epidote-fluid equilibria.

probe analysis revealed very small amounts of Pb and Ni components in sulfide and oxide minerals (as noted above). There can be no question that Pb and Ni in starting oxide, silicate and sulfide phases served as the source of the heterogeneous accumulations of Pb and Ni in alteration phases. Gold crystals were observed in association with the reacted mineral assemblage, which undoubtedly reflects dissolution/re-precipitation of gold from the gold reaction cell, as discussed above.

As expected, aluminosilicate phases failed to show chemical or mineralogical modification. For example, electron microprobe data for epidote and plagioclase solid solutions from the experiment performed at 425 °C, 500 bars and 1.0 molal dissolved Cl^-, reveal little if any differences between starting and reacted compositions, the relatively extreme conditions of the experiment notwithstanding (Table 1, Figs. 2 and 3). Similar analysis of plagioclase and epidote solid solutions from other experiments performed during this study also revealed compositions that do not depart significantly from starting values. That plagioclase solid solution remained An_{70} and indicated virtually no evidence of recyrstallization into a thermodynamically more stable phase is not surprising in light of our previous results with plagioclase solid solutions (Berndt and Seyfried, 1993). That the epidote solid solution also remained unchanged (Ep_{45}) was for us a new finding, but it too is largely in keeping with the well known sluggishness of this phase to equilibrate with aqueous fluids, especially at low to moderate pressures (Liou, 1973). Thus, to accurately assess fluid-mineral equilibria during the experiments, it is essential that constraints imposed by metastable plagioclase and epidote are explicitly taken into account.

4. DISCUSSION

The present study shows that relatively slight changes in temperature, pressure and dissolved Cl^- results in substantial changes in the dissolved concentration of Fe, Cu and other metals in fluids coexisting with a plagioclase-epidote-bearing mineral assemblage. Since plagioclase and epidote solid solutions are abundant phases in natural hydrothermal systems, the results of the experiments can help to constrain pH and redox buffering in these systems. The pH and redox relations of fluids coexisting with these phases, however, depend critically on the relative roles of equilibrium and metastability, which can be evaluated only by assessing mineral solubility simultaneously from both experimental and theoretical perspectives.

In general, results from the present experiments are consistent with data and interpretations from Berndt and Seyfried (1993), in that plagioclase solid solution behaves ideally during fluid-mineral equilibria and

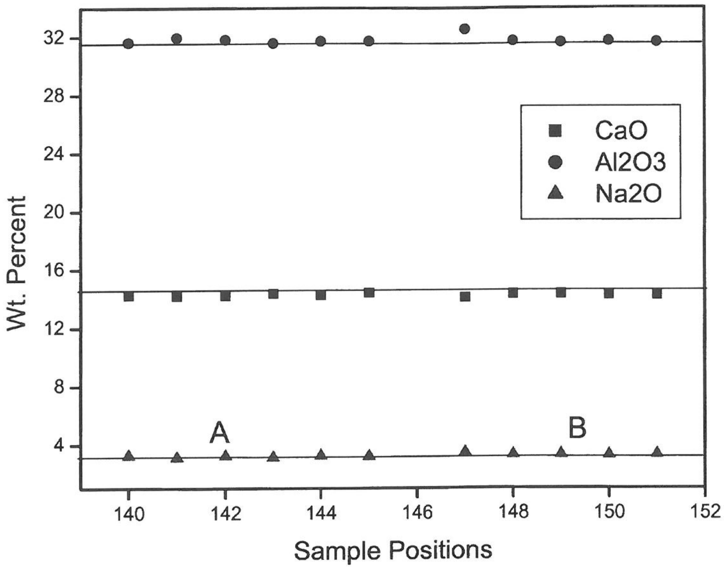

Figure 3. Electron microprobe analyses (CaO, Al_2O_3, Na_2O) of two plagioclase grains (A and B) from a phase equilibria experiment at 425 °C, 500 bars and 1.0 m Cl^-. As with epidote composition, these data reveal compositions ($X_{an} = 0.70$) identical to starting values (solid lines) determined by wet chemical techniques (see text and Table 1). Sample positions refer to transect locations across mineral grains. The data are representative of plagioclase grains from all experiments, and indicate plagioclase metastability during the experiments.

does not recrystallize into a thermodynamically more stable composition, at least on the time scale of the experiments. Thus, the following reaction can be used to depict metastable plagioclase-fluid equilibria:

$$\underset{Anorthite}{CaAl_2Si_2O_8} + 2Na^+ + 4\ \underset{Quartz}{SiO_2} \leftrightarrow \underset{Albite}{2NaAlSi_3O_8} + Ca^{2+} \qquad (2)$$

where the activities of the anorthite and albite components of plagioclase solid solution can be replaced by mole fractions. Even at temperatures and pressures as high as 425 °C and 500 bars, and 1 molal total dissolved Cl^-, dissolved Ca and Na concentrations calculated from equation 2 and appropriate mass-action and mass-balance reactions agree well with experimental data, assuming ideal behavior of anorthite and albite components of An_{70}-plagioclase (Fig. 4a-b). The relative agreement between experimental and theoretical data shown here, however, is, in fact, better than observed by Berndt and Seyfried (1993) for their experiments, which were performed at 400 bars. At 400-425 °C, the higher pressure used for the present experiments (500 bars) minimizes uncertainties in the thermodynamic data for aqueous species estimated using correlation algorithms of Shock and Helgeson (1988), Shock et al. (1989, 1997), and Sverjensky et al. (1997), where pressure effects can be significant, especially at temperatures in the vicinity of the critical temperature of the fluid.

As previously emphasized, the full assemblage of minerals used for the present series of experiments can be shown from theoretical data to buffer completely the dissolved chemistry of the coexisting fluid phase and epidote composition when temperature, pressure, plagioclase composition and total dissolved Cl are fixed. For example, the mole fraction of epidote solid solution predicted, while assuming the ideal site mixing model of Bird and Helgeson (1980a), which explicitly accounts for the temperature dependence of substitutional order-disorder on the octahedral sites, is 0.82 and 0.77 at 425 and 400 °C, respectively. These values, of course, are very different from that of the composition of epidote used for the experiments, which as emphasized, did not reveal evidence of Fe enrichment consistent with theoretical predictions. Thus, for fixed activity of anorthite and epidote components of plagioclase and epidote solid solution respectively, and unit activity for coexisting minerals and water, it can be shown that $a_{Ca^{2+}}/(a_{H^+})^2$ is fixed at any temperature, pressure and dissolved Cl, as follows:

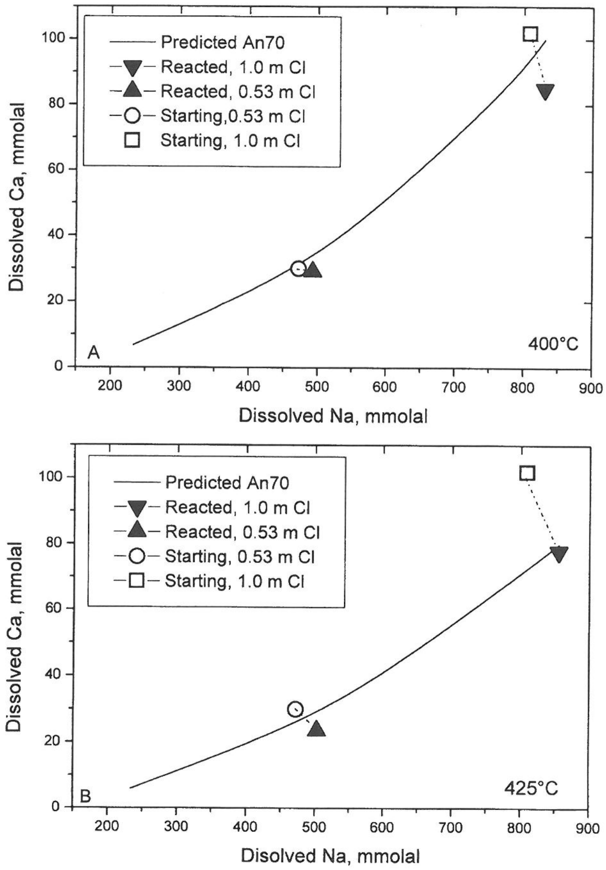

Figure 4. Dissolved Ca concentrations predicted (solid line) and measured (symbols) in fluids coexisting with plagioclase (X_{an} = 0.70)-epidote (X_{ep} = 0.45)-quartz-magnetite-anhydrite-pyrite-chalcopyrite assemblage at 400 (A) and 425 °C (B) 500 bars. Open symbols refer to starting fluid composition, while solid symbols indicate steady-state concentrations. In general, the good agreement between measured and predicted Ca concentrations indicate the important role of metastable mineral-fluid equilibria in controlling fluid chemistry.

Epidote *Pyrite*

$$1.05\,Ca_2Al_2FeSi_3O_{12}(OH) + 2.0\,H^+ + 0.025\,FeS_2 \leftrightarrow$$

Anorthite

$$1.05\,CaAl_2Si_2O_8 +$$

Quartz *Magnetite*

$$1.52\,H_2O + Ca^{2+} + 1.05\,SiO_2 + 0.3573\,Fe_3O_4$$

Anhydrite

$$+ 0.05\,CaSO_4 \qquad (3)$$

In effect, reaction (3), together with imposed constraints (in particular, plagioclase composition, ΣCl^-, and the charge balance equation), buffers fluid pH. Changing the epidote or plagioclase composition, or total dissolved Cl^-, temperature or pressure, will result in a correspondingly different pH value. For example, increases in the anorthite component of plagioclase solid solution (see Berndt et al. 1989; Berndt and Seyfried, 1993), and dissolved Cl^-, decrease pH, while an increase in the epidote component of epidote solid solution (see Bird and Helgeson, 1980a) increases pH. Results of previous experiments (Ding and Seyfried, 1992a) have shown that for a specific redox condition, dissolved Fe concentration is an exceedingly sensitive indicator of pH, and thus can be used here to test the activity of epidote coexisting with plagioclase solid solution at the conditions of the experiments.

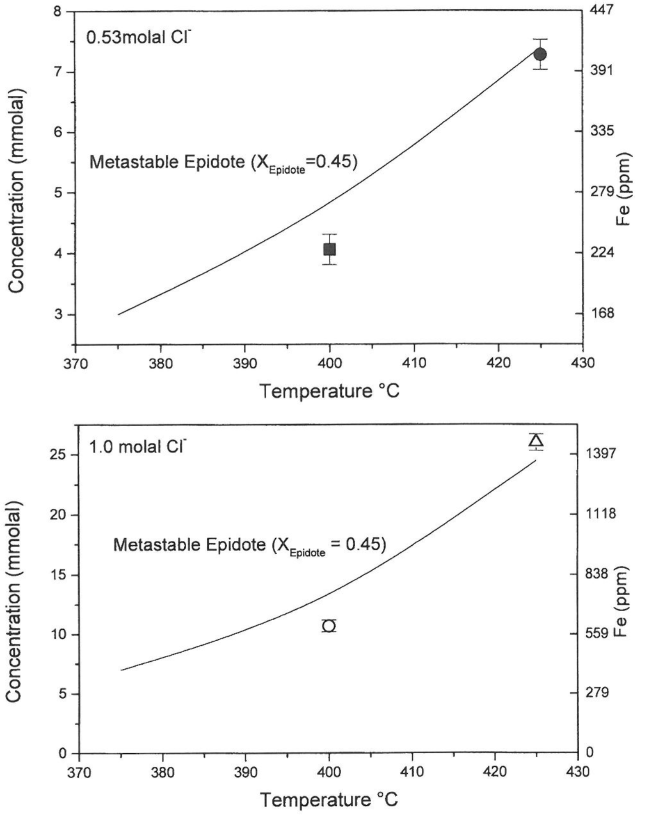

Figure 5. Dissolved Fe concentrations predicted (solid line) and measured (symbols) in 0.53 m total Cl^- (A) and 1.0 m Cl^- (B) coexisting with plagioclase ($X_{an} = 0.70$)-epidote ($X_{ep} = 0.45$)-quartz-magnetite-anhydrite-pyrite-chalcopyrite assemblage at 400 and 425 °C, 500 bars. Symbols refer to steady state concentrations in solution. Data reveal generally good agreement with constraints imposed by metastable epidote ($X_{ep} = 0.45$), rather than an epidote composition ($X_{ep} = 0.77$ to 0.82) formed in full equilibrium with the assemblage of minerals. As developed in the text, relatively low X_{ep} values give rise to relatively low pH values and correspondingly higher metal concentrations (see Fig. 6).

Measured and predicted concentrations of dissolved Fe are depicted in Figure 5, assuming epidote composition equivalent to that of the starting phase as a function of temperature and dissolved Cl^- concentration. It is immediately clear that the measured dissolved Fe, and therefore fluid pH, is entirely consistent with the metastable epidote composition, for both 0.53 m Cl (A) and 1.0 m Cl^- (B) conditions. At 425 °C, 500 bars and 1.0 molal total dissolved Cl^-, the pH values predicted for metastable epidote ($X_{ep} = 0.45$) and predicted ($X_{ep} = 0.82$) compositions are 5.07 and 5.20, respectively (Fig. 6). Although the difference in pH values may appear slight, the corresponding differences in dissolved Fe concentrations are large (Fig. 6). Indeed, a difference in pH (in-situ) of approximately 0.13 results in a 2x variation in dissolved Fe. At temperatures less than 425 °C, model results show that the offset in pH caused by changes in epidote composition (stable vs metastable) decreases largely because the composition of the epidote solid solution predicted to form is less Fe-rich and more like that of the starting metastable phase.

Another test for the pH estimated from fluid-mineral equilibria comes from other dissolved metal concentrations measured during the experiments. For example, Figure 7 shows dissolved Cu concentrations measured and predicted assuming metastable phase equilibria (X_{ep} and X_{an} = 0.45 and 0.70 respectively), together with constraints imposed by chalcopyrite-fluid equilibria at temperatures from 400° to 425 °C, 500 bars, and dissolved Cl^- from 0.53 to 1.0 molal. In general, measured and predicted Cu concentrations are in good agreement, although the measured values exceed those predicted at 425

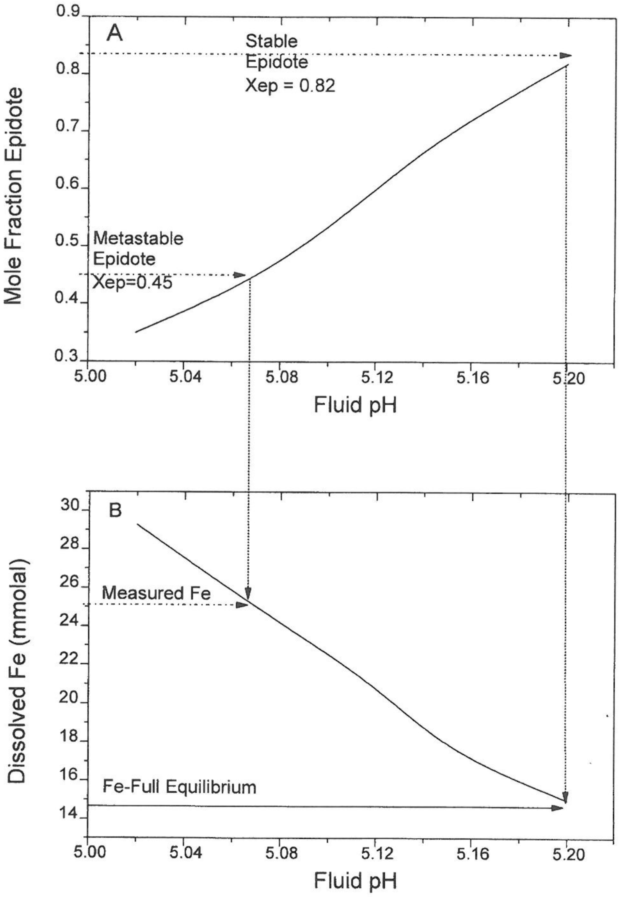

Figure 6. The role of epidote composition on dissolved Fe concentrations and pH (in-situ) of Cl^--bearing aqueous fluid (1.0 m Cl^-) coexisting with plagioclase (X_{an} = 0.70)-epidote-quartz-magnetite-anhydrite-pyrite-chalcopyrite assemblage at 425 °C, 500 bars. The composition of epidote predicted to exist in full equilibrium at experimental conditions departs significantly from that used for the experiment and measured at the termination of the experiment (metastable epidote, X_{ep} = 0.45) (A). The thermodynamically stable epidote composition would give rise to considerably less dissolved Fe (predicted, Fe-Full Equilibrium) than that actually measured (B). In effect, changes in epidote composition result in differences in pH (in-situ), which are responsible for changes in dissolved Fe concentrations.

°C at both dissolved Cl^- conditions. This is likely caused either by uncertainties in the stability constant for $CuCl°_{(aq)}$, which was determined from mineral solubility experiments at conditions very similar to those of the present experiments (Seyfried and Ding, 1993; 1995), or by the existence of another aqueous species of Cu, for which data are presently lacking. It is important to consider, however, that at 425 °C (1.0 molal Cl^-), measured Fe concentration also exceed theoretical predictions, suggesting that at least for this relatively high-temperature-high-Cl^- condition, fluid pH may actually be slightly lower than indicated by metastable mineral-fluid equilibria constraints. A lower pH could be caused by any of a number of factors, but uncertainties in the solid solution models assumed for plagioclase and epidote solid solutions seem most likely. This, coupled with the inherent sensitivity of Cu- and Fe-bearing aqueous species to pH at 400 and 425 °C and 0.53 and 1.0 molal Cl^-, could account for the observed variability. Assuming all of these uncertainties act together to affect pH, a pH variation of as little as 0.02 at 425°C could resolve the apparent offset between predicted and observed metal concentrations. That such a slight adjustment can account for the dissolved concentrations of aqueous species coexisting with such a

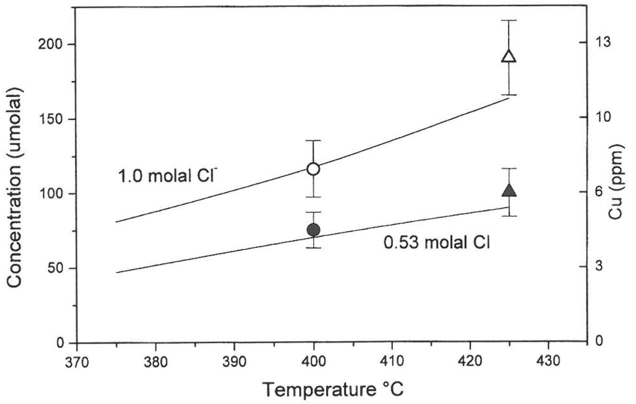

Figure 7. Dissolved Cu concentrations predicted (solid line) and measured (symbols) in fluids (1.0 and 0.53 m total Cl^-) coexisting with plagioclase (X_{an} = 0.70)-epidote (X_{ep} = 0.45)-quartz-magnetite-anhydrite-pyrite-chalcopyrite assemblage at 400 and 425 °C, 500 bars. The slight offset between predicted and measured dissolved Cu concentrations at 425 °C may be due to uncertainties in the distribution of aqueous Cu bearing species or, more likely, slight uncertainties in fluid pH (see text).

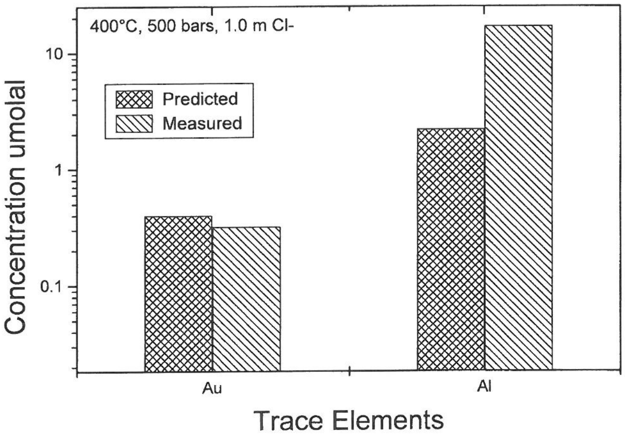

Figure 8. Predicted and measured dissolved concentrations of Au and Al in fluid (umolal) coexisting with plagioclase (X_{an} = 0.70)-epidote (X_{ep} = 0.45)-quartz-magnetite-anhydrite-pyrite-chalcopyrite assemblage at 400 °C, 500 bars and 1.0 molal total dissolved Cl^-. The relative agreement between predicted and measured concentrations for Au lends confidence to pH (in-situ) estimated from constraints imposed by the existence of metastable plagioclase and epidote. The order of magnitude difference between measured and predicted Al concentrations is likely due to uncertainties in Al-speciation at elevated temperatures, pressures and dissolved Cl concentrations.

complex assemblage of minerals at temperatures and dissolved Cl^- concentrations as high as 425 °C and approximately 1.0 molal respectively, is significant indeed, and suggests that, for this chemical system, experimental and theoretical models can be used with a high level of accuracy to constrain a wide range of subseafloor hydrothermal alteration processes. Previously, Seyfried and Ding (1993) used results of experiments in the K_2O-Na_2O-Al_2O_3-SiO_2-Fe_2O_3-FeO-CuO-H_2O-HCl-H_2S system to show that pH values near neutrality at appropriate temperatures and pressure were applicable to hydrothermal reaction zones at mid-ocean ridges. These results are in good agreement with the present

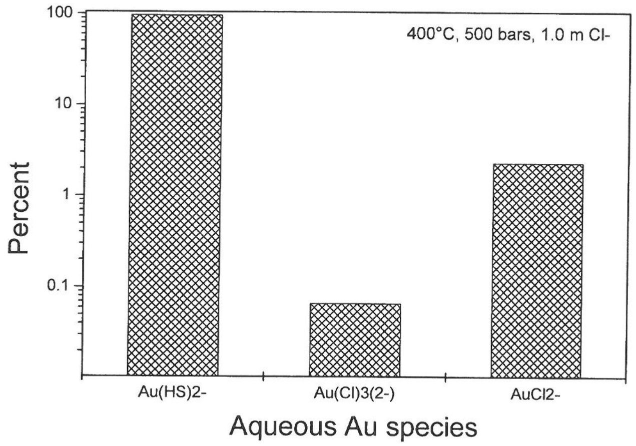

Figure 9. Relative distribution of Au-bearing aqueous species in Cl^- (1.0 molal) and H_2S bearing fluid coexisting with plagioclase ($X_{an} = 0.70$)-epidote ($X_{ep} = 0.45$)-quartz-magnetite-anhydrite-pyrite-chalcopyrite assemblage at 400 °C, 500 bar and 1.0 m Cl^-. Relatively high Cl^- concentrations notwithstanding, Au solubility is dominated by bisulfide species. Thus, changes in dissolved Cl^- concentration in hot spring vent systems are unlikely to affect greatly dissolved Au, although $H_2S_{(aq)}$ effects could be significant, assuming the presence of Au-bearing phases. Thermodynamic data used for the calculations are from SUPCRT92 (Johnson et al., 1992) and Sverjensky et al. (1997)

study using phase relations more applicable to basaltic systems when explicit account is taken of the effect of mineral metastability on the pH of coexisting aqueous fluids.

Taking this same approach one step further, we can evaluate the general agreement between theoretical and experimental data for Au, Al and Pb at a particular temperature, pressure and dissolved Cl^- concentration, which may also help to constrain in-situ pH values, again assuming metastable fluid-mineral equilibria. For example, we have already established that gold was among the alteration products observed at the end of the experiments, and certainly existed throughout the experiment, since the experimental reactants were held within the gold reaction cell. Thus, it is likely that pH-dependent gold-fluid equilibria controlled dissolved Au during the experiments. Similarly, Al activity was likely fixed by alumino-silicate phases (plagioclase/epidote solid solutions), and thus, assuming knowledge of the distribution of dissolved Al species at experimental conditions, Al concentration can also be used to constrain pH.

At a temperature and dissolved Cl^- concentration of 400 °C and 1.0 molal, where data are most complete (Table 4), there is in fact good agreement between predicted and measured concentrations of dissolved gold, although the same is not true for dissolved Al (Fig. 8). Assuming pH is not the problem, as indicated by Fe and Cu data, together with dissolved Au, then the relatively high measured concentrations of Al suggest the existence of aqueous Al complexes other than simple hydroxyl species - all that is available in the recently revised SUPCRT database (Shock et al., 1997; Sverjensky et al., 1997). Indeed, it may be that at the conditions of the experiments, alkali bearing Al-complexes (Anderson, 1995), or other Al-bearing aqueous species (Pokrovski et al. 1996) enhance the solubility of the Al-bearing minerals. Other than the relatively high Al concentration measured for the first sample from the experiment at 400 °C, 500 bars (0.53 m Cl), the experimental data are also in generally good agreement with the range of Al concentrations reported for hot spring vent fluids at mid-ocean ridges. For example, end-member Al concentrations recently measured for vents at EPR 9-10°N (Von Damm, personal communication), range from approximately 5 to 18 μmolal. These data also reveal a slight positive correlation with dissolved Cl, suggesting some form of chlorocomplexing. Although still preliminary, it is significant that the highest dissolved Al concentration (18 μmolal) is associated with the more Cl-rich vent fluid (850 mmolal), a value which is also in good agreement with results from our 1.0 molal Cl-experiments, suggesting the existence of a Cl-complex of Al in the experiments. Without more data from experiments at lower dissolved Cl^- concentrations, it is not possible to test unambiguously the role of Cl^- and temperature on Al-speciation effects, although this may be one the few occasions where field data are used to constrain

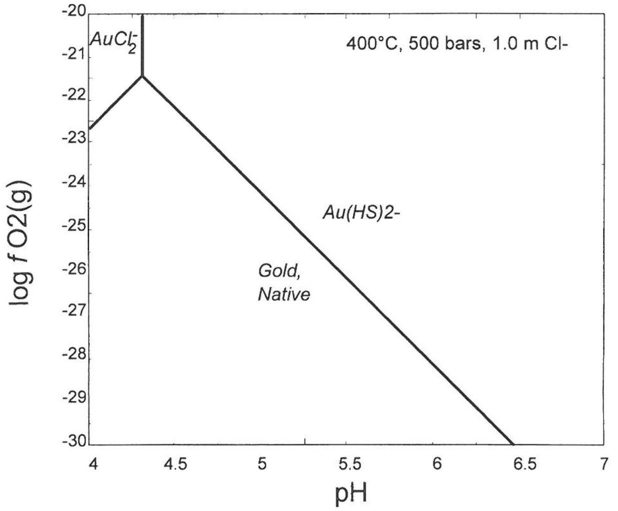

Figure 10. pH-log $f_{O_{2(g)}}$ diagram for the Au-HCl-H_2S-H_2O system at 400 °C, 500 bars and 1.0 molal total dissolved Cl depicting the predominance of Au-bearing species and native gold. H_2S and Au activity are fixed at values consistent with measured concentrations of these species at experimental conditions (Table 4). Calculations were performed with EQ3/EQ6 (Wolery and Daveler, 1992) taking explicit account of activity/concentration relations, and appropriate mass balance, charge balance and mass action expressions. Thermodynamic data used for the calculations are from SUPCRT92 (Johnson et al., 1992) and Sverjensky et al. (1997).

experimental results, and generally shows the benefits of an integrated approach to the study of mineral-fluid interaction at elevated temperatures and pressures.

In apparent contrast with Al, bisulfide complexes are predicted to dominate the distribution of Au-bearing species in fluids coexisting with the metastable plagioclase-epidote-bearing mineral assemblage (Fig. 9). This is important, because it suggests that pH increase and increases in total dissolved H_2S may be more critical than dissolved Cl in contributing to the mobility of gold in subseafloor hydrothermal systems. Of course, it is unlikely that the activity of Au in the submarine hydrothermal system is buffered by native gold, but whichever phase does control gold, this phase would likely respond to changes in fluid chemistry in ways very different than Cu- and Fe-bearing minerals (or even Al-phases), where chloro-complexing is so important in the mobility of these species (Fe and Cu) at elevated temperatures and pressures (Crerar and Barnes, 1976; Hemley et al., 1992; Ding and Seyfried, 1992a,b). To illustrate this better, we can make use of an activity ($f_{O_{2(g)}}$ vs pH) diagram for the Au-H_2S-HCl-H_2O-NaCl system, which shows that at 400 °C, 500 bars and 1.0 molal Cl^-, together with an activity of $H_2S_{(aq)}$ equivalent to that of the experiments at the described conditions, all but the most oxidizing and acidic conditions, $Au(HS)_2{}^-{}_{(aq)}$ is the predominate aqueous species of gold (Fig. 10).

For the same range of conditions (400 °C, 500 bars, 1.0 molal total dissolved Cl^-), Pb solubility can be calculated to be dominated by chloro-complexes, in particular, $PbCl_{2(aq)}$, which represents over 75% of the total dissolved Pb. Thus, assuming the presence of Pb-bearing phases in subseafloor hydrothermal systems, it is likely that dissolved Pb will correlate with dissolved Cl, like dissolved Fe and Cu, and anti-correlate with pH. Although dissolved Pb data are generally lacking for vent fluids from unsedimented portions of ridges, data that are available for fluids from EPR 9-10°N (Von Damm, personal communication), reveal concentrations on the order of 2 μmolal, in reasonable agreement with values observed here, but nearly a factor of 500 times lower than galena-controlled Pb concentrations.

Metastable plagioclase-epidote-fluid equilibria with imposed constraints not only fix pH, and constrain the mobility of dissolved metals, but when taken together with coexisting oxide and sulfide phases, also fix $f_{O_{2(g)}}$, as follows:

Anorthite *Anhydrite* *Quartz* *Magnetite*

$$CaAl_2Si_2O_8 + 0.5H_2O + CaSO_4 + SiO_2 + 0.5Fe_3O_4$$

Epidote *Pyrite*

$$\leftrightarrow CaAl_2FeO_{12}(OH) + 1.75O_{2(g)} + 0.5FeS_2 \quad (4)$$

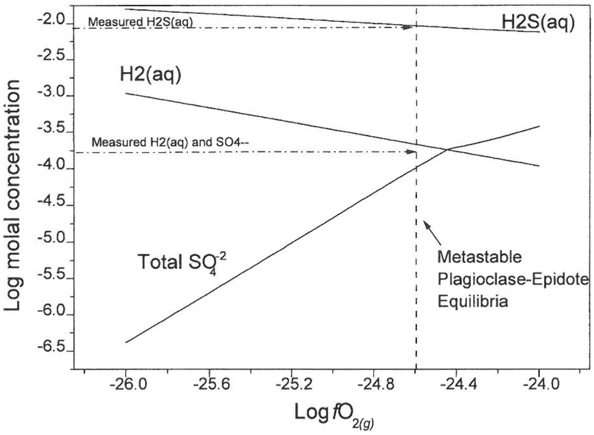

Figure 11. Predicted and measured dissolved sulfur species and $H_{2(aq)}$ in fluid coexisting with plagioclase (X_{an} = 0.70)-epidote (X_{ep} = 0.45)-quartz-magnetite-anhydrite-pyrite-chalcopyrite assemblage at 400 °C, 500 bar and 0.53 total dissolved Cl^- as a function of log $f_{O_2(g)}$. $m_{H_2S(aq)}$ is in very good agreement with theoretical predictions taking account of salting-out effects in NaCl fluid (Ding and Seyfried, 1990) and data from Kishima (1989). Measured H_2 and SO_4^{2-} are slightly below and above theoretical predictions, respectively. Overall agreement is still good, and indicates the potential usefulness of dissolved sulfur species and H_2 in vent fluids as a means of constraining redox in subseafloor reaction zones at mid-ocean ridges.

For example, at 400 °C, 500 bars and 0.53 m Cl^-, a log $f_{O_2(g)}$ of –24.59 can be calculated assuming activities of anorthite and epidote components of plagioclase and epidote solid solutions consistent with measured constraints (Fig. 11). Also plotted on Figure 11 are changes in the dissolved concentrations of total SO_4^{2-}, $H_{2(aq)}$ and $H_2S_{(aq)}$ predicted as a function of changes in log $f_{O_2(g)}$, which also can be compared with values of these species actually measured during the experiment. Data indicate that predicted concentrations of $H_{2(aq)}$ and $H_2S_{(aq)}$ increase with decreasing $f_{O_2(g)}$, whereas the opposite is true for total dissolved SO_4^{2-}. Furthermore, a decrease of log $f_{O_2(g)}$ of a single unit below experimental conditions causes SO_4^{2-} to decrease by approximately two log units. Measured concentrations of $H_{2(aq)}$ and $H_2S_{(aq)}$ are in good agreement with theoretical predictions, although measured SO_4^{2-} exceeds the value predicted by approximately a factor of 2. The relatively slight off-set in predicted and measured concentrations of dissolved SO_4^{2-} notwithstanding, the data reveal that $H_{2(aq)}$ and the $H_2S_{(aq)}/SO_4^{2-}$ ratio can provide internally consistent indicators of redox relations in fluid coexisting with mineral assemblages at temperatures from 400 to 425 °C, and provide an alternative to dissolved H_2 or m_{Fe}/m_{Cu} ratio (see Seyfried and Ding, 1993) as proxies for redox in subseafloor reaction zones, assuming seawater entrainment during vent fluid sampling can be effectively accounted for. Over-determination of redox by combining approaches, however, provides valuable insight on reaction zone conditions, and characteristics such as temperature, pressure, mineralogy, and mineral composition may be determined with much greater accuracy and confidence than presently available by any single approach, providing even greater insight on the temporal evolution of hydrothermal reactions at mid-ocean ridges. This approach could be especially valuable at a hydrothermal system such as TAG, where subseafloor mixing between seawater and vent fluid can result in local redox gradients, which can be discerned better by application of multiple redox proxies.

Another way to visualize the effect of mineral equilibria on the distribution of redox-dependent aqueous species at experimental conditions (e.g., 400 °C, 500 bars, 0.53 m Cl^-) is by use of an activity-activity diagram for the FeO-Fe_2O_3-Al_2O_3-SiO_2-CaO-H_2O-HCl-H_2S system (Fig. 12). Indeed, it can be seen here that for an $a_{Ca^{2+}}/(a_{H^+})^2$ ratio consistent with metastable plagioclase (X_{an} = 0.7)-epidote (X_{ep} = 0.45) equilibria (5.34, see previous discussion), $a_{H_2S(aq)}$-$a_{H_2(aq)}$ for fluid coexisting with anhydrite, pyrite and magnetite, plots at a point on the pyrite-magnetite boundary that is relatively close to the HMP (Hematite-Magnetite-Pyrite) invariant point. In general, for all conditions to the right of the dashed line in Figure 12, anhydrite is unstable, and SO_4^{2-}

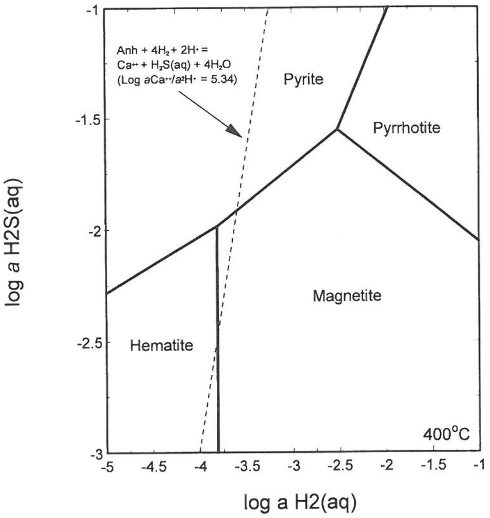

Figure 12. Log $a_{H_2S_{(aq)}}$-log $a_{H_{2(aq)}}$ diagram depicting the anhydrite stability field for fluid coexisting with plagioclase (X_{an} = 0.70)-epidote (X_{ep} = 0.45)-quartz-magnetite-pyrite-chalcopyrite assemblage at 400 °C, 500 and 0.53 molal total dissolved Cl^-. For imposed constraints, the "anhydrite-in" boundary is located near the hematite-magnetite-pyrite (HMP) invariant, but considerably removed from the pyrite-pyrrhotite-magnetite (PPM) invariant. Whether or not the anhydrite-bearing assemblage buffers redox in vent fluids depends largely on the extent of fluid/rock interaction. Hydrothermal systems with very low fluid/rock mass ratios might not be able to eliminate igneous pyrrhotite from controlling redox, while high fluid/rock mass ratios may render pyrite unstable, which would be manifest by a decrease in H_2S, although H_2 may still be relatively high (see text). Thermodynamic data used for the calculations are from SUPCRT92 (Johnson et al., 1992).

converts to $H_2S_{(aq)}$. Changes in $a_{Ca^{2+}}/(a_{H^+})^2$ values, which can result from changes in the activity of anorthite or epidote components of plagioclase and epidote solid solution respectively, can, however, cause some movement of the "anhydrite-in" boundary. For example, an anorthite activity lower than 0.7 would cause this boundary to move to the right in Figure 12, while the opposite would be true for a decrease in the activity of epidote solid solution (e.g., see reaction 3). Owing to constraints imposed by anhydrite stability, however, relatively large changes in the composition/activity of the alumino-silicate assemblage result in only minor changes in the position of the anhydrite stability field (all else being held constant). Thus, stable or metastable equilibria involving plagioclase and epidote solid solutions coexisting with anhydrite, pyrite and magnetite and a Cl—bearing aqueous fluid will likely define a relatively restricted region in $H_2S_{(aq)}$ space, which makes this species in vent fluids a more reliable indicator of redox in subseafloor hydrothermal alteration processes. Of course, changes in temperature, pressure, dissolved Cl^- (salting-out), together with changes in phase assemblage, will exert considerable influence on this, and seafloor applications must explicitly consider any or all of these possibilities to interpret accurately $H_2S_{(aq)}$ concentrations in hot spring vent fluids. Again, it is for this reason, that application of multiple redox constraints are most useful.

4.1. Mineral-fluid Equilibria and Subseafloor Reaction Zones at Mid-Ocean Ridges: Redox Constraints.

Concentrations of dissolved H_2S in vent fluids decrease sharply with decreasing dissolved Cl (Fig. 13). Cl^- variations, of course, are largely the result of phase separation of seawater derived fluid into vapor- and brine-rich components (Bischoff and Rosenbauer, 1987), while $H_2S_{(aq)}$ variations reflect phase equilibria in subseafloor reaction zones, which can also be influenced by Cl^- owing to salting-out effects, as discussed earlier. For example, assuming a reaction zone temperature and pressure of 400 °C and 500 bars, dissolved $H_2S_{(aq)}$ can be predicted from the present study to decrease from approximately 12 to 6 mmolal with increase in Cl from 300 to 1000 mmolal, respectively. Lower temperatures (e.g., 375 °C) result in lower $H_2S_{(aq)}$ concentrations. The effect of Cl^- on $H_2S_{(aq)}$ at the lower temperature is also less owing to temperature-dependent changes in the Setchenow co-

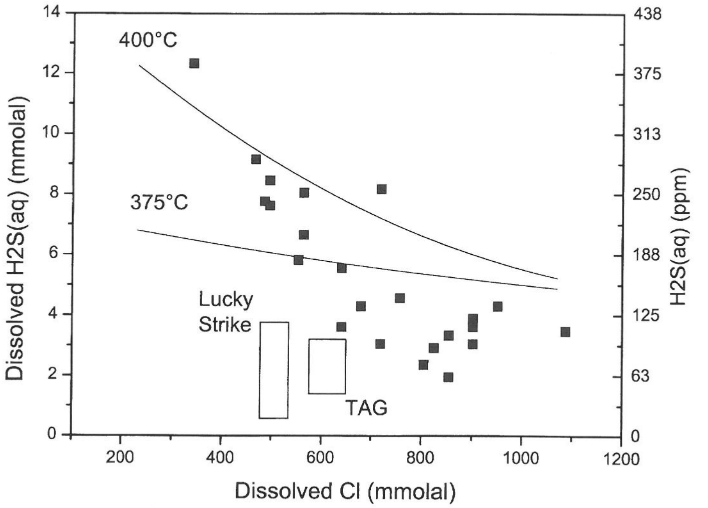

Figure 13. Dissolved $H_2S_{(aq)}$ vs Cl^- concentrations of selected vent fluids at mid-ocean ridges (Von Damm, 1995 and references therein) in comparison with $H_2S_{(aq)}$ concentrations in fluid coexisting with plagioclase (X_{an} = 0.70)-epidote (X_{ep} = 0.45)-quartz-magnetite-anhydrite-pyrite-assemblage at 375-400 °C, 500 bars. The relatively low $H_2S_{(aq)}$ concentrations of many vent fluids may indicate re-equilibration at temperatures less than 375 °C, which is likely the case with the very high-salinity fluids, where temperatures of venting fluid may be as low as 220 °C (see text). In contrast, the conspicuously low $H_2S(aq)$ concentration for vent fluids at Lucky Strike (Von Damm et al., 1998) and TAG (Edmond et al. 1995; Tivey et al., 1995), suggests the loss of pyrite from the reaction zone mineral assemblage (see Fig. 12). This scenario is very much in keeping with the relatively low m_{Fe}/m_{Cu} ratio for the TAG vent fluids (Allen and Seyfried, 1998). Availability of experimentally calibrated theoretical data allows rigorous constraints to be placed on the mineralogic composition of subseafloor reaction zones at mid-ocean ridges.

efficient of $H_2S_{(aq)}$ (Ding and Seyfried, 1990) and the ionic strength of NaCl-fluid. That vent fluids with dissolved Cl^- near seawater values approach H_2S concentrations consistent with phase equilibria constraints involving the anhydrite-bearing system of minerals at 375-400 °C, suggests similar conditions in subseafloor reaction zones. The sharply lower $H_2S_{(aq)}$ concentrations of the high-Cl^- fluids, however, most likely reflect the effects of more extreme cooling, which may be caused by the high density of these fluids precluding rapid ascent to the seafloor. Indeed, the unusually high-Cl^- vent fluids at SJDF ridge have measured temperatures of only 220-290 °C indicating extensive conductive cooling (Von Damm and Bischoff, 1987) with likely attendant loss in $H_2S_{(aq)}$. In cases such as this, it is difficult to constrain unambiguously reaction-zone conditions. Vent fluids at Lucky Strike (Von Damm et al., 1998) and at TAG (Edmond et al. 1995; Tivey et al., 1995), however, are not only characterized by low $H_2S_{(aq)}$ concentrations, but also by low to moderate dissolved Cl^- concentrations (Fig. 13), and relatively high temperatures (Edmond et al., 1995; Tivey et al., 1995; Von Damm et al., 1998), which makes it unlikely that post-reaction zone cooling can account for the relatively low H_2S concentrations for these hydrothermal systems.

An alternative explanation for the relatively low H_2S concentrations at Lucky Strike, TAG, and for similar systems, may involve other chemical and physical factors related to fluid/rock mass ratio and the composition of the substrate through which the hydrothermal fluids circulate. For example, it is well known from the relatively low concentrations of trace incompatible elements in fluids at these sites that fluid/rock mass ratios are relatively high (Von Damm et al., 1998; Campbell et al., 1988b). The reasons for this are likely complex, but could result from tectonic activity that could enhance fluid flow along high-permeability channels, ultimately creating a highly altered substrate. Considering the relatively high solubility of pyrite in aqueous fluids at elevated temperatures, it is likely that the H_2S inventory of the substrate would be effectively depleted in a relatively short period of time, with a corresponding decrease in the concentration of H_2S in the coexisting fluid phase. In effect, the proposed loss of pyrite as a reactant would destroy the H_2S-buffer capacity of the mineral assemblage, and further reaction progress would result in a relatively sharp decrease in H_2S, but only a modest change in H_2 (Fig. 12). That dissolved $H_{2(aq)}$ at TAG (Charlou et al., 1996) is nearly identical to the values measured here at 400 °C, 500 bars (Table 3), is consistent with this interpretation. In addition to accounting for relatively low $H_2S_{(aq)}$, the loss of pyrite in subseafloor reaction zones at TAG, would result in a decrease in m_{Fe}/m_{Cu} ratio, in a manner very much equivalent to what is observed (Allen and Seyfried, 1998).

Whether or not the scenario outlined above to account for the relatively low $H_2S_{(aq)}$ concentrations in hydrothermal fluids at TAG and elsewhere is accurate can not be assessed unambiguously without additional experimental data for an expanded chemical system, at a wider range of temperatures and especially for fluid pressures less than 500 bars. What is clear, however, is that the strategy of conducting experiments to calibrate theoretical models, and then using the models to constrain hydrothermal alteration processes, represents a valuable approach to assess controls on the chemistry of hot spring vent fluids. Indeed, only by use of an integrated approach involving field, experimental and theoretical data can real progress be made in our ability to understand the temporal evolution of exceedingly complex and often metastable chemical systems that characterize subseafloor reaction zones at mid-ocean ridges.

5. SUMMARY AND CONCLUSIONS

Chemical reactions between circulating hydrothermal fluids of seawater origin and rocks of basaltic composition commonly involve metastable mineral assemblages that contain plagioclase solid solutions at temperatures > 400 °C, and low to moderate pressures. The persistence of mineral metastability, however, together with phase separation processes in the NaCl-H_2O system, which can cause substantial changes in total dissolved Cl^- concentrations of coexisting aqueous fluids, can create an exceedingly complex chemical environment, one that may be may be difficult to model thermodynamically. The present investigation, therefore, was conducted to assess the relative agreement between results of experimental and theoretical models depicting phase relations in the $CaO\text{-}Na_2O\text{-}Al_2O_3\text{-}SiO_2\text{-}Fe_2O_3\text{-}FeO\text{-}CuO\text{-}HCl\text{-}H_2O\text{-}H_2S$ system at temperatures from 400-425 °C, 500 bars pressure and dissolved Cl^- concentrations from 0.53 to 1.0 molal. Although experiments were performed at lower pressures (300-500 bars), the dearth of reliable thermodynamic data for aqueous species effectively precludes comparison with experimental results for the relatively low-pressure range of conditions.

In general, for conditions for which comparisons can be made, there is good agreement between experimental and theoretical data when explicit account is made for the presence of metastable phases. Previous experimental data documented this for plagioclase solid solutions, but it is clear from the present investigation that epidote solid solution, a primary component of the starting mineral assemblage, also maintains its composition at initial values, and quite distinct from that which is predicted from phase equilibria constraints. Whereas metastable plagioclase is best indicated by dissolved concentrations of Na and Ca, epidote metastability is revealed by pH effects, which under experimental conditions are manifest by variability of dissolved metal concentrations, especially Fe. For example, at 425 °C, 500 bars and 1.0 molal total dissolved Cl^-, recrystallization of the starting epidote ($X_{ep} = 0.45$) to a thermodynamically more stable phase ($X_{ep} = 0.82$), would give rise to a relatively high-pH fluid and correspondingly low dissolved Fe concentrations. That the measured Fe gives a pH nearly equivalent to that in metastable equilibrium with the starting epidote composition ($X_{ep} = 0.45$), confirms this interpretation, as do electron microprobe data which fail to show compositional modification of the starting epidote.

Dissolved Cu, fixed by the presence of chalcopyrite, and Au, fixed by the gold reaction cell, require a pH (in-situ) that is consistent with the presence of metastable epidote ($X_{ep} = 0.45$). Dissolved Al concentrations, however, depart sharply from predicted values, suggesting the existence of more complex distribution of Al species than are included in the available thermodynamic database. The experimentally measured Al, however, is in reasonably good agreement with vent fluid data suggesting similar speciation in natural systems. This point notwithstanding, the generally good agreement between predicted and measured dissolved metal concentrations confirms that plagioclase and epidote solid solutions coexisting with Na-Ca-Cl fluids can provide a valuable means of buffering pH of fluids at elevated temperatures and pressures. Although this can be important to pH control in subseafloor hydrothermal systems, it is also important to the design of hydrothermal experiments where pH control is often critically needed to assess unambiguously a wide range of reaction processes. That pH can be changed and maintained simply by changing epidote composition, offers many advantages to alternative approaches.

Dissolved sulfur species and measured $H_{2(aq)}$ concentrations are also consistent with redox constraints imposed in part by metastable epidote-plagioclase-fluid equilibria. In this case, however, it can be shown that for the anhydrite-bearing system, $H_2S_{(aq)}$ is relatively insensitive to compositional variability of the alumino-silicate assemblage, as is the Fe/Cu ratio, two parameters that have been used in vent fluids to constrain redox in subseafloor reaction zones. Although many vent fluids with dissolved Cl^- concentrations near seawater have $H_2S_{(aq)}$ concentrations consistent with a reaction zone mineral assemblage containing metastable plagioclase-epidote, together with quartz, magnetite, anhydrite, and pyrite, this does not appear to be the case for systems having higher dissolved Cl^- concentrations where either distinctly lower temperatures or different phase relations are suggested. It is clear that additional experiments and modeling calculations are needed over a wider range of conditions and with more diverse phase assemblages to distinguish between these two possibilities. The need for additional experiments is underscored further by the fact that the chemistry of many vent fluids is influenced greatly by critical phenomena in the NaCl-H_2O system, which is largely unsupported by theoretical data because this is an exceedingly challenging region of pressure-temperature-composition space. Experiments, however, must also include explicit consideration of mineral kinetics and recrystallization effects, so as to assess better the temporal evolution of minerals and fluids from complex natural systems.

Acknowledgements—We thank Meg Tivey and Scott Wood for their comments and suggestions that greatly improved the final version of the manuscript. We would also like to acknowledge the many helpful discussions with Mike Berndt and Doug Allen, which played an important role in the development of the concepts reflected in the paper. This research was supported by NSF grants: OCE-9605441, OCE-9633132, and OCE-98188908.

Editorial handling: Scott A. Wood

REFERENCES

Allen D. E. and Seyfried W. E. Jr. (1998) Phase equilibria constraints on the chemistry of sub-seafloor reaction zones at 400°C, 500 bars and 1 molal Cl. *Abstracts with Programs - Geological Society of America*, 29, n. 6, p. 25.

Anderson G. M. (1995) Is there alkali-aluminum complexing at high temperatures and pressures? *Geochim. Cosmochim. Acta* **59**, 2155-2161.

Berndt M. E. and Seyfried W. E. Jr. (1993) Calcium and sodium exchange during hydrothermal alteration of calcic plagioclase at 400°C and 400 bars. *Geochim. Cosmochim. Acta* **57**, 4445-4453.

Berndt M. E., Seal R. R. II, Shanks W. C. III, and Seyfried W. E. Jr. (1996) Hydrogen isotope systematics of phase separation in submarine hydrothermal systems: Experimental calibration and theoretical models. *Geochim. Cosmochim. Acta.* **60**, 1595-1604.

Berndt M. E., Seyfried W. E. Jr., and Janecky D. R. (1989) Plagioclase and epidote buffering of cation ratios in mid-ocean ridge hydrothermal fluids: Experimental results in the near supercritical region. *Geochim. Cosmochim. Acta* **53**, 2283-2300.

Bird D. K. and Helgeson H. C. (1980a) Chemical interaction of aqueous solutions with epidote-feldspar mineral assemblages in geologic systems. 1. Thermodynamic analysis of phase relations in the system CaO-FeO-Fe_2O_3-Al_2O_3-SiO_2-H_2O-CO_2. *Am. Jour. Sci.* **280**, 907-941.

Bird D. K. and Helgeson H. C. (1980b) Chemical interaction of aqueous solutions with epidote-feldspar assemblages in geologic systems. II. Equilibrium constraints in the metamorphic/geothermal process. *Amer. J. Sci.* **281**, 576-614.

Bischoff J. L. and Rosenbauer R. J. (1987) Phase separation in seafloor geothermal systems: An experimental study on the effects of metal transport. *Amer. J. Sci.* **287**, 953-978.

Bowers T. S., Campbell A. C., Measures C. I., Spivack A. J., and Edmond J. M. (1988) Chemical controls on the composition of vent fluids at 13°-11°N and 21°N, East Pacific Rise. *J. Geophys. Res.* **93**, 4522-4536.

Butterfield D. A. and Massoth G. J. (1994) Geochemistry of North Cleft Segment Vent Fluids - Temporal Changes in Chlorinity and Their Possible Relation to Recent Volcanism. *J. Geophys. Res-Solid. Earth.* **99**, 4951-4968.

Butterfield D. A., McDuff R. E., Mottl M. J., Lilley M. D., Lupton J. E., and Massoth G. J. (1994) Gradients in the composition of hydrothermal fluids from the Endeavor segment vent field: Phase separation and brine loss. *J. Geophys. Res.* **99**, 9561-9583.

Campbell A. C., Bowers T. S., and Edmond J. M. (1988a) A time-series of vent fluid compositions from 21°N, EPR (1979, 1981, and 1985) and the Guaymas Basin, Gulf of California (1982, 1985). *J. Geophys. Res.* **93**, 4537-4549.

Campbell A. C., Palmer M. R., Klinkhammer G. P., Bowers T. S., Edmond J. M., Lawrence J. R., Casey J. F., Thompson G., Humphris S., Rona P., and Karson J. A. (1988b) Chemistry of hot springs on the Mid-Atlantic Ridge. *Nature* **335**, 514-519.

Charlou J. L., Donval J. P., Jean-Baptiste P., Dapoigny A., and Rona P. A. (1996) Gases and helium isotopes in high temperature solutions sampled before and after ODP Leg 158 drilling at TAG hydrothermal field (26 degrees N, MAR). *Geophysical Research Letters* **23**, 3491-3494.

Chen C.-T. A. and Marshall W. L. (1982) Amorphous silica solubilities; IV, Behaviour in pure water and aqueous sodium chloride, sodium sulfate, magnesium chloride, and magnesium sulfate solutions up to 350 degrees C. *Geochim. Cosmochim. Acta* **46**, 279-287.

Crerar D. A. and Barnes H. L. (1976) Ore solution chemistry V. Solubilities of chalcopyrite and chalcocite assemblages in hydrothermal solution at 200° to 350°C. *Econ. Geol.* **71**, 772-794.

Ding K. and Seyfried W. E. Jr. (1989) H_2 and H_2S concentrations as indicators of temperature in ridge crest hydrothermal systems. *EOS, Trans. Amer. Geophys. Union* **70**, 1397.

Ding K. and Seyfried W. E. Jr. (1990) Activity coefficients of H_2 and H_2S in NaCl solutions at 300-425°C, 300-500 bars with application to ridge crest hydrothermal systems. *EOS, Trans. Amer. Geophys. Union* **71**, 1680.

Ding K. and Seyfried W. E. Jr. (1992a) Determination of Fe-Cl Complexing in the Low Pressure Supercritical Region (NaCl Fluid) - Iron Solubility Constraints on pH of Subseafloor Hydrothermal Fluids. *Geochim. Cosmochim. Acta.* **56**, 3681-3692.

Ding K. and Seyfried W. E. Jr. (1992b) Experimental determination of Cu-Cl speciation at the T-P conditions relevant to ridge crest hydrothermal activity: Implications to log f_{O_2} in hot spring fluids. *EOS, Trans. Amer. Geophys. Union* **73**, 254.

Edmond J. M., Campbell A. C., Palmer M., Klinkhammer G. P., German C. R., Edmonds H. N., Elderfield H., Thompson G., and Rona P. (1995) Time series studies of vent fluids from the TAG and MARK sites (1986, 1990) Mid-Atlantic Ridge: A new solution chemistry model and mechanism for Cu/Zn zonation in massive sulfide ore deposits. In *Hydrothermal Vents and Processes*, Vol. 87 (ed. L. M. Parson, C. L. Walker, and D. R. Dixon), pp. 411. Geological Society Special Publication.

Fornari D. J., Shank T., Von Damm K. L., Gregg T. K. P., Lilley M., Levai G., Bray A., Haymon R. M., Perfit M. R., and Lutz R. (1998) Time-series temperature measurements at high-temperature hydrothermal vents, East Pacific Rise 9 degrees 49'-51'N; evidence for monitoring a crustal cracking event. *Earth Planet. Sci. Lett.* **160**, 419-431.

Helgeson H. C. (1969) Thermodynamics of hydrothermal systems at elevated temperatures and pressures. *Amer. J. Sci.* **267**, 729-804.

Helgeson H. C., Kirkham D. H., and Flowers G. C. (1981) Theoretical prediction of the thermodynamic behavior of aqueous electrolytes at high pressures and temperatures. IV. Calculation of activity coefficients, osmotic coefficients, and apparent molal and standard and relative partial molal properties to 600°C and 5 kb. *Amer. J. Sci.* **281**, 1249-1516.

Hemley J. J., Cygan G. L., Fein J. L., Robinson G. R., and D'Angelo W. M. (1992) Hydrothermal ore-forming processes in light of studies in rock buffered systems: I. Iron, copper, lead, zinc sulfide solubility relations. *Econ. Geol.* **87**, 1-22.

Johnson J. W., Oelkers E. H., and Helgeson H. C. (1992) SUPCRT92 - A Software Package for Calculating the Standard Molal Thermodynamic Properties of Minerals, Gases, Aqueous Species, and Reactions from 1-Bar to 5000-Bar and 0-Degrees-C to 1000-Degrees-C. *Computers & Geosciences.* **18**, 899-947.

Kishima N. (1989) A thermodynamic study on the pyrite-pyrrhotite-magnetite-water system at 300-500 C with relevance to the fugacity/concentration quotient of aqueous H_2S. *Geochim. Cosmochim. Acta* **53**, 2143-2155.

Liou J. R. (1973) Synthesis and stability relations of epidote, $Ca_2Al_2FeSi_3O_{12}(OH)$. *J. Petrol.* **14**, 381-413.

Orville P. M. (1972) Plagioclase cation exchange equilibria with aqueous chloride solution: results at 700°C and 2000 bars in the presence of quartz. *Amer. J. Sci.* **272**, 234-272.

Pokrovski G. S., Schott, J., Harrichoury, J.-C., and Sergeyev A. S. (1996) The stability of aluminum silicate complexes in acidic solutions from 25 to 150°C *Geochim. Cosmochim. Acta* **60**, 2495-2503.

Saccocia P. J. and Seyfried W. E. Jr. (1990) Talc-quartz equilibria and the stability of magnesium chloride complexes in NaCl-$MgCl_2$ solutions at 300, 350, and 400°C, 500 bars. *Geochim. Cosmochim. Acta* **54**, 3283-3295.

Seewald J. S. and Seyfried W. E. Jr. (1990) The effect of temperature on metal mobility in subseafloor hydrothermal systems: Constraints from basalt alteration experiments. *Earth Planet. Sci. Lett.* **101**, 388-403.

Seyfried W. E. Jr., Janecky D. R., and Berndt M. E. (1987) Rocking autoclaves for hydrothermal experiments II. The flexible reaction cell system. In *Hydrothermal Experimental Techniques* (ed. H. L. Barnes and G. C. Ulmer), pp. 216-240. Wiley Interscience.

Seyfried W. E. Jr. and Ding K. (1993) The effect of redox on the relative solubilities of copper and iron in Cl-bearing aqueous fluids at elevated temperatures and pressures: An experimental study with application to subseafloor hydrothermal systems. *Geochim. et Cosmochim. Acta* **57**, 1905-1917.

Seyfried W. E. Jr. and Ding K. (1995) Phase equilibria in subseafloor hydrothermal systems: A review of the role of redox, temperature, pH and dissolved Cl on the chemistry of hot spring fluids at mid-ocean ridges. In *Seafloor Hydrothermal Systems: Physical, Chemical, Biologic and Geological Interactions*, Vol. Geophysical Monograph 91 (ed. S. E. Humphris, R. A. Zierenberg, L. S. Mullineaux, and R. E. Thompson), pp. 248-273. American Geophysical Union.

Seyfried W. E. Jr. Ding K., and Berndt M. E. (1991) Phase equilibria constraints on the chemistry of hot spring fluids at mid-ocean ridges. *Geochim. Cosmochim. Acta* **55**, 3559-3580.

Shanks W. C. III, Boehlke J. K., Seal, R. R. II. (1995) Stable isotopes in mid-ocean ridge hydrothermal systems; interactions between fluids, minerals, and organisms. *Seafloor hydrothermal systems; physical, chemical, biological, and geological interactions.* Vol. Geophysical Monograph 91 (ed. S. E. Humphris, R. A. Zierenberg, L. S. Mullineaux, and R. E. Thompson), pp. 248-273. American Geophysical Union.

Shock E. L. and Helgeson H. C. (1988) Calculation of the thermodynamic and transport properties of aqueous species at high pressures and temperatures: Correlation algorithms for ionic species and equation of state predictions to 5 kb and 1000°C. *Geochim. Cosmochim. Acta* **52**, 2009-2036.

Shock E. L. and Helgeson H. C. (1990) Calculation of the thermodynamic and transport properties of aqueous species at high pressures and temperatures: Standard partial molal properties of organic species. *Geochim. Cosmochim. Acta* **54**, 915-945.

Shock E. L., Helgeson H. C., and Sverjensky D. A. (1989) Calculations of the thermodynamic and transport properties of aqueous species at high pressures and temperatures: Standard partial molal properties of inorganic neutral species. *Geochim. Cosmochim. Acta* **53**, 2157-2183.

Shock E. L., Sassani D. C., Willis M., and Sverjensky D. A. (1997) Inorganic species in geologic fluids: Correlations among standard molal thermodynamic properties of aqueous ions and hydroxide complexes. *Geochim. Cosmochim. Acta* **61**, 907-950.

Sverjensky D. A., Hemley J. J., and D'Angelo W. M. (1991) Thermodynamic assessment of hydrothermal alkali feldspar-mica-aluminosilicate equilibria. *Geochim. Cosmochim. Acta* **55**, 989-1005.

Sverjensky D. A., Shock E. L., and Helgeson H. C. (1997) Prediction of the thermodynamic properties of aqueous metal complexes to 1000 degrees C and 5 kb. *Geochim Cosmochim Acta* **61**(7), 1359-1412.

Tanger J. C. and Helgeson H. C. (1988) Calculation of the thermodynamic properties of aqueous species at high pressure and temperatures: Revised equation of state for the standard partial properties of ions and electrolytes. *Amer. J. Sci.* **288**, 19-98.

Tivey M. K., Humphris S. E., Thompson G., Hannington M. D., and Rona P. A. (1995) Deducing patterns of fluid flow and mixing within the TAG active hydrothermal mound using mineralogical and geochemical data. *J Geophys*

Res Solid Earth **100**(B7), 12527-12555.

Von Damm K. L., Edmond J. L., Grant B., Measures C. I., Walden B., and Weiss R. F. (1985) Chemistry of submarine hydrothermal solutions at 21°N, East Pacific Rise. *Geochim. Cosmochim. Acta* **49**, 2221-2237.

Von Damm K. L. (1988) Systematics of and postulated controls on submarine hydrothermal solution chemistry. *J. Geophys. Res.* **93**, 4551-4562.

Von Damm K. L. (1995) Controls on the chemistry and temporal variability of seafloor hydrothermal fluids. In *Seafloor Hydrothermal Systems: Physical, Chemical, Biologic and Geologic Interactions*, Vol. Geophysical Monograph 91 (ed. S. E. Humphris, R. A. Zierenberg, L. S. Mullineaux, and R. E. Thompson), pp. 222-248. American Geophysical Union.

Von Damm K. L. and Bischoff J. L. (1987) Chemistry of hydrothermal solutions from the southern Juan De Fuca Ridge. *J. Geophys. Res.* **92**, 11,334-11,346.

Von Damm K. L., Bray A. M., Buttermore L. G., and Oosting S. E. (1998) The geochemical controls on vent fluids from the Lucky Strike vent field, Mid-Atlantic Ridge. *Earth Planet. Sci. Lett.* **160**, 521-536.

Von Damm K. L., Buttermore L. G., Oosting S. E., Bray A. M., Fornari D. J., Lilley M. D., and Shanks W. C. I. (1997) Direct observation of the evolution of a seafloor 'black smoker' from vapor to brine. *Earth Planet. Sci. Lett.* **149**, 101-111.

Wolery T. J. and Daveler S. A. (1992) EQ6, A computer program for reaction path modeling of aqueous geochemical systems: Theoretical manual, users guide, and related documentation (version 7.0). **UCRL-MA-110662 PT IV**, 1-337.